

Electrochemical detection of cefiderocol for therapeutic drug monitoring

Journal Article**Author(s):**

McLeod, James; Stadler, Ellen; Wilson, Richard; Holmes, Alison; O'Hare, Danny

Publication date:

2021-12

Permanent link:

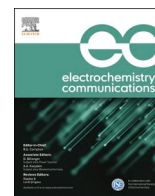
<https://doi.org/10.3929/ethz-b-000513806>

Rights / license:

[Creative Commons Attribution-NonCommercial-NoDerivatives 4.0 International](#)

Originally published in:

Electrochemistry communications 133, <https://doi.org/10.1016/j.elecom.2021.107147>



Full Communication

Electrochemical detection of cefiderocol for therapeutic drug monitoring

James McLeod^{a,b,*}, Ellen Stadler^{b,c}, Richard Wilson^a, Alison Holmes^{a,d}, Danny O'Hare^b^a Centre for Antimicrobial Optimisation, Imperial College London, Hammersmith Hospital, W12 0NN, UK^b Department of Bioengineering, Imperial College London, London SW7 2AZ, United Kingdom^c Department of Information Technology and Electrical Engineering, ETHZ, Zürich 8092, Switzerland^d National Institute for Health Research Health Protection Research Unit in Healthcare Associated Infections and Antimicrobial Resistance, Imperial College London, UK

ARTICLE INFO

Keywords:

Antimicrobial resistance
Cefiderocol

ABSTRACT

Cefiderocol is a novel siderophore-conjugated β -lactam antibiotic which has been approved for clinical use. It has demonstrated efficacy against infections caused by Gram-negative bacteria, including carbapenem-resistant strains. Novel antibiotics are rarely brought to market and, as such, are ideal candidates for therapeutic drug monitoring which enables optimised dosing across a range of clinical scenarios whilst also reducing the chances of antimicrobial resistance. Here we demonstrate direct electrochemical detection of cefiderocol by oxidation using untreated gold and glassy carbon electrodes as well as multi-walled carbon nanotube (MWCNT)-coated glassy carbon and foamed gold electrodes. Quantification of cefiderocol in the therapeutic range is demonstrated in spiked whole human blood using MWCNT-coated pyrolytic carbon screen-printed electrodes.

1. Introduction

Antimicrobial resistance develops in nature due to selection, allowing populations of microbes to protect themselves from toxic substances. For example, beta lactamase, an enzyme which deactivates beta lactams such as penicillin, has existed in nature for millions of years [1]. In human medicine, for antimicrobials to be effective they have to be at a concentration above a minimum inhibitory concentration (MIC) [2], "the lowest concentration which resulted in maintenance or reduction of inoculum viability" [3]. Below this concentration, the antimicrobial will still act as a selection pressure on the microbes, increasing the chance of resistance developing [4]. Selecting a dosage that maintains blood concentrations above the MIC, while avoiding toxicity, is therefore hugely important. This, however, is not straightforward. Therapeutic drug monitoring is not only relevant in respect to drugs with a narrow therapeutic index, but is also important due to large inter- and inpatient variations in pharmacokinetics, making the standardisation of dosing difficult [5].

New antibiotics, such as cefiderocol, are developed very infrequently: only three new antimicrobial drugs were approved by the FDA in 2019 alongside cefiderocol [6]. Globally around 700,000 people a year die from antimicrobial-resistant infections and this number could rise to 10 million a year by 2050 [7]. Analytical methodology can play a large part in protecting the efficacy of these vital treatments [8] and the

low cost and ease of miniaturisation of electrochemical methods makes them ideal candidates for point-of-care monitoring and dose optimisation.

Cefiderocol is a novel siderophore-conjugated cephalosporin antibiotic developed by Shionogi & Co. Ltd. Its combination of a catechol siderophore with a cephalosporin core has led to a drug with potent *in vitro* activity against carbapenem-resistant and multidrug-resistant Gram-negative bacteria [9]. The drug has been approved for the treatment of Gram-negative infections in several countries, including the USA, which has approved the use of cefiderocol for the treatment of hospital-acquired bacterial pneumonia and ventilator-associated pneumonia caused by Gram-negative bacteria. The susceptibility breakpoint standard provided by the Clinical and Laboratory Standards Institute (CLSI) is $\leq 4\mu\text{g}/\text{mL}$ ($\leq 5.3\mu\text{M}$) against *Enterobacteriales*, *P. aeruginosa*, and *Acinetobacter* spp., and $\leq 1\mu\text{g}/\text{mL}$ ($\leq 1.3\mu\text{M}$) against *S. maltophilia* [10].

Here we propose a novel electrochemical sensor for the direct electrochemical detection of cefiderocol for use as a point-of-care sensor for therapeutic drug monitoring. The electrochemical behaviour of cefiderocol was studied at unmodified glassy carbon electrodes using cyclic voltammetry (CV). Calibration curves were subsequently obtained by differential pulse voltammetry (DPV) for a range of electrodes with surface modifications. Performance in whole blood was evaluated in the therapeutic range for MWCNT pyrolytic carbon electrodes.

* Corresponding author at: Centre for Antimicrobial Optimisation, Imperial College London, Hammersmith Hospital, W12 0NN, UK.

E-mail address: jrm215@ic.ac.uk (J. McLeod).<https://doi.org/10.1016/j.elecom.2021.107147>

Received 24 August 2021; Received in revised form 13 October 2021; Accepted 15 October 2021

Available online 20 October 2021

1388-2481/© 2021 Published by Elsevier B.V. This is an open access article under the CC BY-NC-ND license (<http://creativecommons.org/licenses/by-nc-nd/4.0/>).

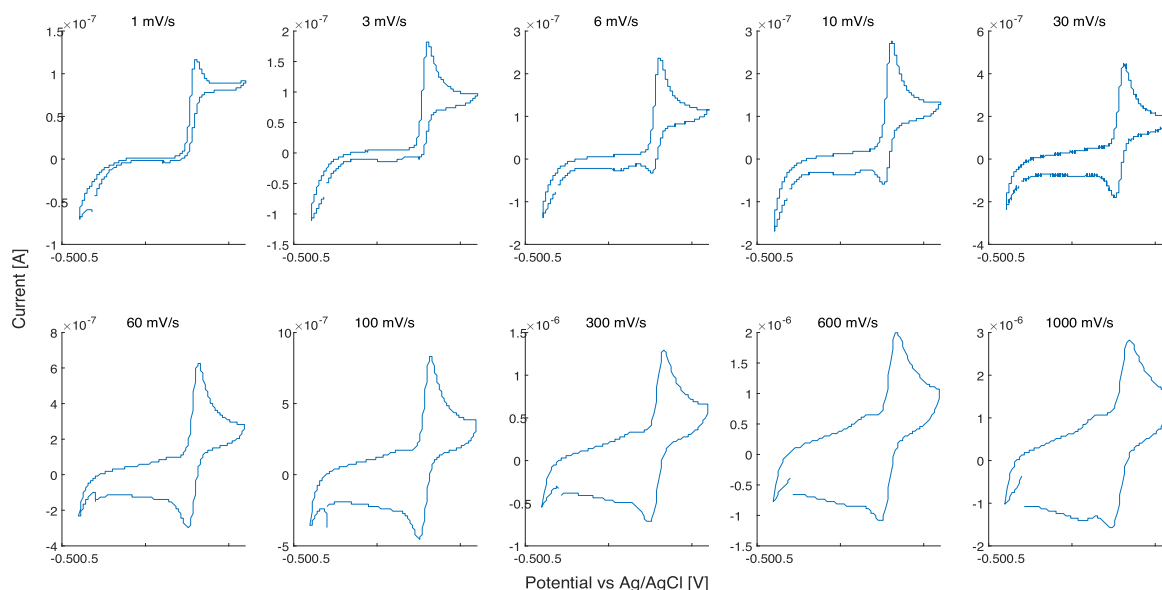


Fig. 1. Cyclic voltammograms of 100 μM cefiderocol on unmodified glassy carbon electrodes at a variety of scan rates in 7.4 pH 0.1 M PBS solution.

2. Materials and methods

2.1. Materials

All chemicals were procured from Sigma Aldrich unless specified otherwise. Cefiderocol was provided by Shionogi & Co. Ltd.

Gold and glassy carbon working electrodes, silver–silver chloride reference electrodes ($\text{Ag}|\text{AgCl}|\text{NaCl}(\text{aq})$ (3 M)) against which all potentials are reported, and platinum counter electrodes were purchased from CH Instruments.

Pyrolytic carbon disposable electrodes were purchased from Respire Diagnostics Ltd.

2.2. Electrode preparation

Gold electrodes and glassy carbon electrodes (GCEs), 3 mm in diameter, were first polished sequentially with aqueous alumina slurry, starting at an average size of 1 μm , followed by 0.3 μm , then 0.05 μm . They were then sonicated in aqueous detergent (Decon) solution and rinsed thoroughly in de-ionised water.

Electrochemical cleaning was performed by cycling 1000 times between -0.4 and -1.35 V against a $\text{Ag}|\text{AgCl}|\text{NaCl}(\text{aq})$ (3 M) electrode at 2 V s^{-1} in aqueous 0.5 M NaOH. The electrodes were then rinsed thoroughly with de-ionised water, before being transferred to 0.5 M H_2SO_4 and cycled between -0.35 and 1.5 V for 20 cycles at 4 V s^{-1} and for 4 cycles at 0.1 V s^{-1} [11].

2.3. Modified electrodes

Foamed gold electrodes were prepared by electrodeposition from a solution of 0.1 M HAuCl_4 and 2 M NH_4Cl at a potential of -4 V for 20 s against a $\text{Ag}|\text{AgCl}|\text{NaCl}(\text{aq})$ (3 M) electrode with a platinum counter electrode [12]. This forms a series of pores of increasing size, producing a honeycomb-like structure with a hugely increased surface area by electroplating gold around a scaffold of hydrogen bubbles [12].

For the multi-walled carbon nanotube (MWCNT)-modified electrodes, 1 mg/ml of carbon nanotubes was added to a 0.05% (w/v) solution of Nafion in ethanol and sonicated to obtain a well-dispersed

suspension. 5 μL of the suspension was pipetted onto the prepared glassy carbon electrodes, or pyrolytic carbon disposable electrodes (Respire Diagnostics) and left to dry for 30 min at room temperature [13] before use.

Thorough characterization of the pyrolytic carbon disposable electrodes can be found on the Respire Diagnostics website [14].

2.4. Electrochemical methods

Electrochemical measurements were conducted using a three-electrode cell with either carbon or gold electrodes as the working electrode (as above), a platinum wire electrode as the counter electrode and a $\text{Ag}|\text{AgCl}|\text{NaCl}(\text{aq})$ (3 M) reference electrode. Cyclic voltammetry and differential pulse voltammetry were carried out on an Ivium CompactStat potentiostat. Measurements were carried out at 22.5 ± 1 degrees.

2.5. Blood sample collection

Sample collection was approved by the London-Harrow Research Ethics Committee (reference 19/LO/0219). Samples were collected from healthy volunteers (who were not taking any medication) via a cannula, with the first 3 ml of blood taken being discarded. Samples were combined with EDTA to stop clotting and used immediately.

3. Results and discussion

3.1. Electrode mechanism

To investigate the electrochemical properties of cefiderocol on unmodified glassy carbon electrodes, cyclic voltammetry was performed with scan rates ranging from 1 to 1000 mV s^{-1} in phosphate-buffered saline (PBS) containing 100 μM cefiderocol. Well-defined anodic and cathodic peaks are present at 0.21 V and 0.19 V respectively (Fig. 1), which are not found in a blank solution (see Fig S1 in the supplementary information), indicating that the peak represents the oxidation of cefiderocol on the GCE. For further analysis of the reaction occurring at the electrode surface, the diffusion gradient at the electrode must not be

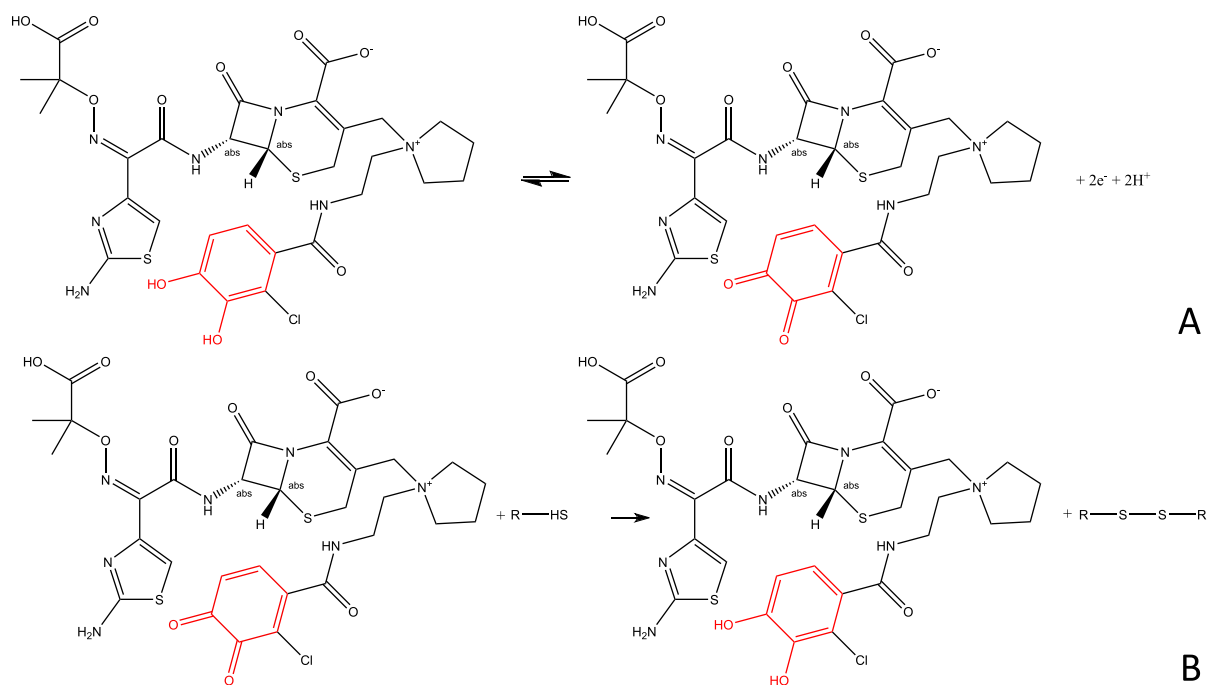


Fig. 2. Proposed reaction mechanisms for (A) electrochemical oxidation of cefiderocol and (B) regeneration of cefiderocol from its oxidised form by reaction with albumin.

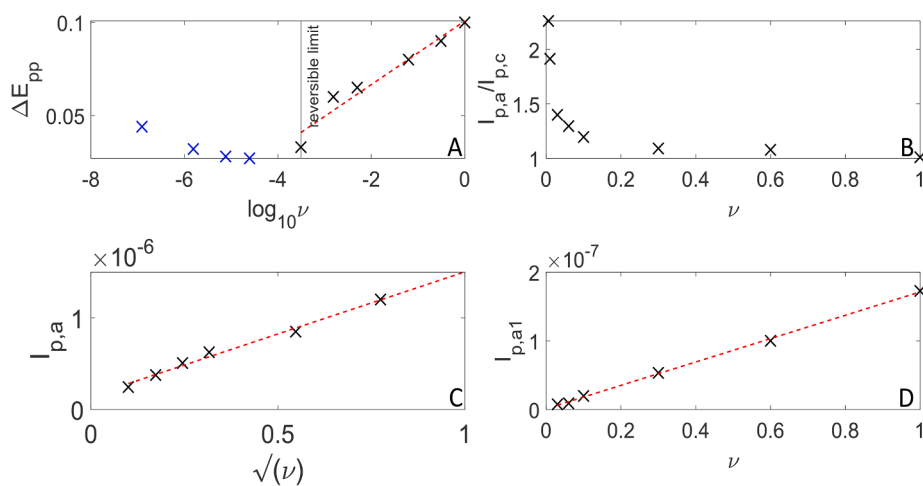


Fig. 3. The effect of scan rate on (A)–(C) the principal redox peaks and (D) the minor adsorbed peaks. (A) Peak separation as a function of scan rate; (B) anodic to cathodic peak current ratio ($I_{p,a}/I_{p,c}$) versus scan rate; (C) anodic peak current versus the square-root of the scan rate; (D) anodic peak heights of the minor peaks occurring around 0.1 V ($I_{p,a1}$) versus scan rate.

affected by the natural convection boundary layer (approximately 0.05 cm [15]). This sets a lower limit to the scan rate of 30 mV s^{-1} (estimated diffusion coefficient of cefiderocol is $5 \times 10^{-10} \text{ m}^2 \text{ s}^{-1}$). At scan rates above 30 mV s^{-1} additional peaks appear at 0.1 and 0.05 V. These peak currents scale linearly with scan rate (Fig. 3D), which is a characteristic of adsorbed redox processes. These minor peaks appear to be due to the absorption of an electroactive species that we have not identified [16]. Adsorption pre-waves can be excluded since adsorbed cefiderocol in the absence of the solution phase drug does not show this redox couple (see below). An initial potential of -0.3 V was used since these additional minor peaks could not be clearly distinguished when starting at 0 or -0.4 V .

Fig. 2 shows the proposed reaction mechanism for the oxidation of cefiderocol in PBS (A) and the regeneration of cefiderocol from its

oxidised form by reaction with reduced cysteine residues in albumin (B), the predominant plasma protein. Chemically reversible rapid electron transfer reactions are typically observed for catechols [17]. Additionally, the one-electron product can oligomerise, and the quinoid can oxidise other species e.g. the cysteine moiety on albumin, or be subject to 1,4 addition (Michael) by nucleophiles [18].

The intended clinical use of this detection method is as a point-of-care sensor which can detect the concentration of cefiderocol in a drop of serum or blood. This adds complicating factors [19] such as the presence of approximately 4% (w/w) albumin [20] in human plasma and its adsorption and denaturation on the electrode surface [21,22]. Potential effects of albumin adsorption include: electrode blocking, diffusional barriers, analyte partitioning, changes in chemical composition of the electrode/electrolyte interface arising from the Donnan

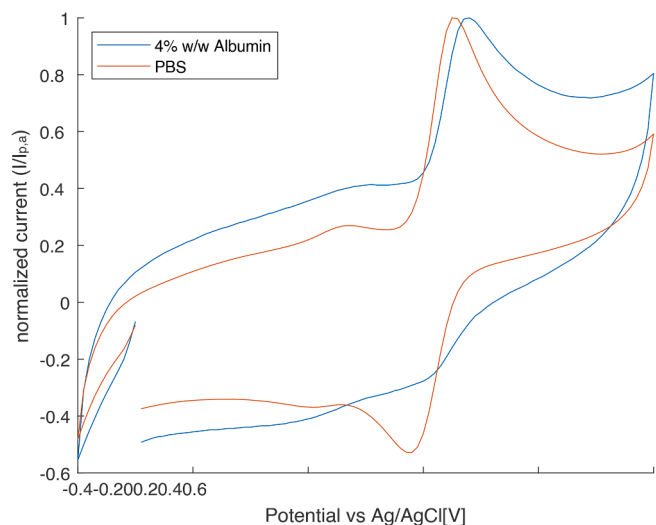


Fig. 4. Cyclic voltammograms of 100 μM cefiderocol in PBS with and without the addition of 4% w/w albumin. Peak currents are normalised against the peak anodic current. Scan rate 100 mV s^{-1} .

equilibrium, blocking of adsorption and electrocatalytic sites which are typically promiscuous, and chemical or catalytic reactions with the electrode reaction product. This latter phenomenon has been observed for ferricyanide and dopamine in previous studies of electrode biofouling [23]. Comparison with dopamine results suggests the possibility of catalytic regeneration of the catechol moiety by reaction with cysteine residues in the adsorbed protein.

The relationship between the peak-to-peak potential (ΔE_{pp}) and the logarithm of the scan rate ($\log_{10} \nu$) (Fig. 3A) shows that the reaction can be considered quasi-reversible. The difference between peak and half peak height was used to assess the number of electrons transferred in the electrochemical reaction [24]. A peak potential separation of 0.045 V at a scan rate of 0.3 Vs^{-1} and assuming the transfer coefficient $\alpha = 0.5$ gives $n = 2.13$, consistent with the proposed reaction mechanism in Fig. 2. A decrease in the anodic to cathodic peak current ratio ($I_{p,a}/I_{p,c}$) with increasing scan rate (Fig. 3B) suggests that the reduced form of cefiderocol is consumed in a homogeneous chemical reaction. For scan rates $> 100 \text{ mV s}^{-1}$ the peak current ratio is unity. In this case, therefore,

the characteristic time of the electrochemical method τ is small compared to the characteristic lifetime $t_{1/2}^{\text{chem}}$ of the chemical reaction with rate constant k_{EC} . With $\tau = \frac{RT}{F\nu}$ for cyclic voltammetry and $t_{1/2}^{\text{chem}} = \frac{1}{k_{\text{EC}}}$ for a first-order reaction, we conclude that the coupled homogeneous reaction has a rate constant $k_{\text{EC}} < 4\text{s}^{-1}$ [24].

A plot of the square root of the scan rate against the principal anodic peak current reveals a linear relationship consistent with a diffusion-controlled process (Fig. 3C) [25,26] with analytical utility. Background currents were subtracted from the peak currents for this analysis.

Fig. 4 shows the cyclic voltammograms, normalised to the anodic peak current, of 100 μM cefiderocol in PBS and PBS with 4% (w/w) bovine serum albumin (scan rate 100 mV s^{-1}). Here the catechol moiety is regenerated from the oxidised quinone moiety by reaction with the cysteine groups on the albumin as proposed in Fig. 2, decreasing the relative size of the reduction peak current (Fig. 4). These CVs were carried out with a starting potential of -0.3 V , scanning initially towards -0.4 V . This was done to preserve the small peaks between 0 and 0.1 V. With an initial potential of 0 or -0.4 V , these peaks were partially obscured by the capacitive charging current.

3.2. Nanostructured electrodes

Modification of electrode surfaces with nanostructures frequently offers the analytical advantage of enhanced sensitivity [27]. Indeed, anodic peak currents for 100 μM cefiderocol in 4% BSA were significantly higher for a MWCNT-Nafion-coated GCE than for Nafion-coated and untreated GCEs over a range of scan rates (Fig. 5A). MWCNTs have multiple edges which are largely occupied by oxygen functionalities which can enhance both adsorption and electron transfer rates. The presence of the MWCNTs can also introduce thin-layer behaviour [28].

Three different processes could contribute to the enhanced response of the nanostructured electrode [29]:

- (1) increased electrocatalytic activity could lead to a larger effective rate constant k_0 , which results in an increase in the current by the ratio of reversible to irreversible peak currents in the Randles-Sevcik equation;
- (2) thin-layer behaviour of the analyte in any porous layer formed by MWCNTs could lead to higher peak currents which would be proportional to the scan rate;

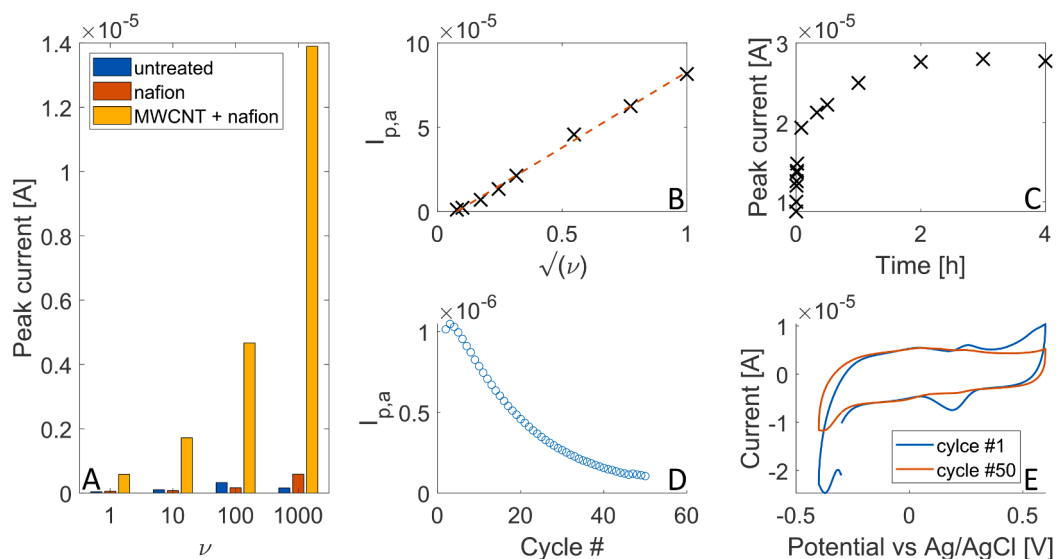


Fig. 5. (A) Cyclic voltammetric anodic peak currents in PBS at three different stages of the MWCNT modification; (B) plot of current against the square root of scan rate for the modified electrode; (C) DPV peak current of an MWCNT-modified electrode against time in 4 μM cefiderocol solution. (D) Peak currents in PBS against CV cycles for a MWCNT electrode previously exposed to cefiderocol solution. (E) Example of the CVs used to remove adsorbed analyte.

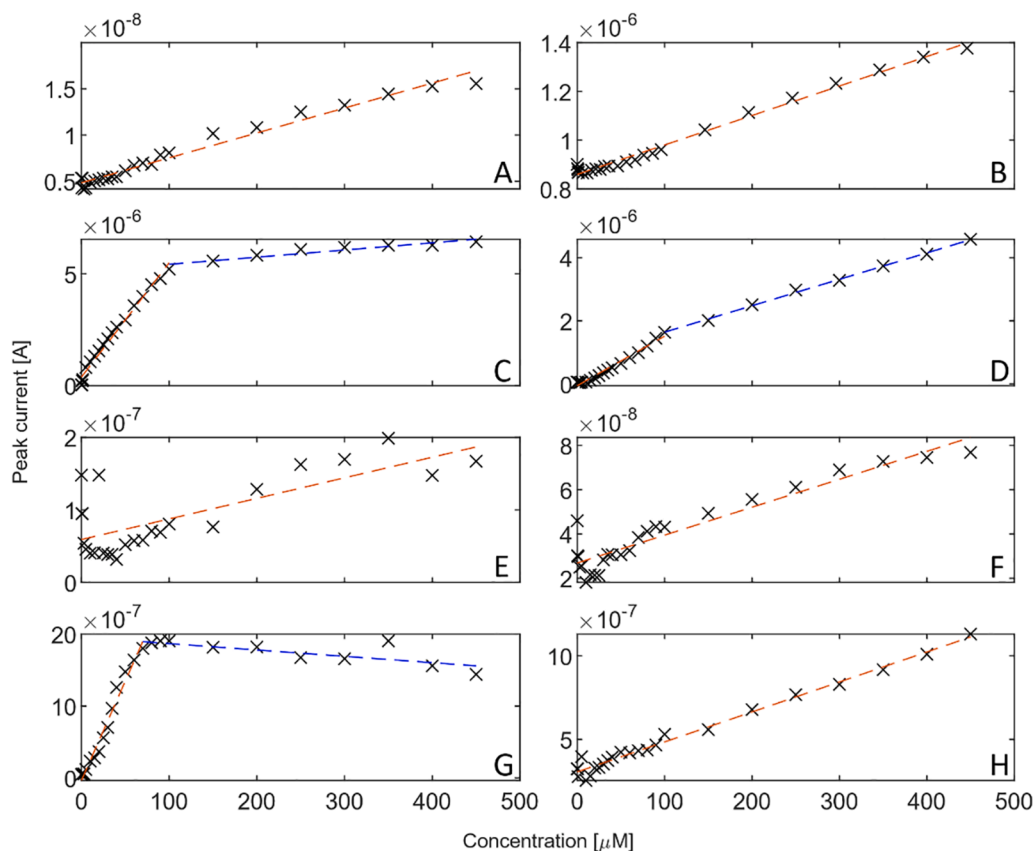


Fig. 6. Calibration curves for cefiderocol on (A) glassy carbon electrode in PBS; (B) glassy carbon in 4% albumin; (C) MWCNT in PBS; (D) MWCNT in 4% albumin; (E) gold in PBS; (F) bulk gold in 4% albumin; (G) foamed gold in PBS; (H) foamed gold in 4% albumin.

(3) enhanced extent of diffusion-limited adsorption arising from the increased electrode area and changed geometry.

The relative contributions of these three processes can be evaluated voltammetrically. The increased peak currents for the MWCNT-modified electrodes cannot be accounted for solely by a putative increased heterogeneous rate constant. A plot of the square root of the scan rate versus the anodic peak current, Fig. 5B, reveals a linear relationship, indicating that the overall reaction at the electrode is diffusion controlled and the contribution to the current of the analyte in solution is large compared to the contribution of the analyte trapped in the MWCNT layer for the scan rates examined [30].

To investigate analyte adsorption, a MWCNT-coated GCE was left in a solution of 4 μM cefiderocol in PBS for 4 h. At different timepoints (10, 20, 30, 40, 50, 60 s, 5, 20, 30 min and 1, 2, 3 and 4 h), the electrode was rinsed thoroughly with PBS before obtaining a DPV curve in PBS. Clear peaks were observed, indicating analyte adsorption. The peak current increased for two hours (Fig. 5C). As suggested by Huang and co-workers, the adsorbed analyte can be removed from the MWCNT-nanotube electrode between measurements by repeated cycles in the background analyte until the oxidation peaks disappear [31]. 50 CV scans were conducted on the electrode and the anodic peak currents were plotted against the number of cycles (Fig. 5D). This confirmed that the oxidation peaks due to adsorbed material on the electrode disappeared after 50 CV cycles (Fig. 5E); MWCNT GCE electrodes can be cleaned in supporting electrolyte by CV after each measurement. The peak potentials were consistent with the major peaks in cefiderocol solution, showing that the minor peaks cannot be attributed to adsorption pre-waves.

3.3. Calibration curves

Initially calibration curves were generated for plain gold and carbon electrodes in PBS solution. DPV scans were carried out from 0 to 0.4 V with a pulse time of 10 ms, a pulse amplitude of 50 mV, a potential step of 1 mV and a scan rate of 50 mV s^{-1} . Nitrogen-purged PBS was spiked with cefiderocol and the peak heights at around 0.2 V were plotted against cefiderocol concentration. The sensitivity of the carbon and gold electrodes were $28.05 \times 10^{-6} \text{ A/M}$ and $136 \times 10^{-6} \text{ A/M}$, respectively (see Fig. 6A and E). The gold electrode however proved ineffective at concentrations below 100 μM .

Calibration was then repeated using the nanostructured electrodes, the carbon nanotube-modified electrodes, and the foamed gold electrodes. The Nafion layer is thin (approximately 250 nm) and serves to bind the carbon nanotubes into place. The voltammetric responses of the bare GC and Nafion-coated GC closely resembled each other (see Fig S2 in the supplementary information).

Fig. 6C and G show DPV calibration curves for the carbon nanotube-modified electrodes and the foamed gold electrodes in PBS. Their sensitivity is greatly increased compared with the unmodified electrodes, with a sensitivity of $47.0 \times 10^{-3} \text{ A/M}$ for carbon nanotubes and $26 \times 10^{-3} \text{ A/M}$ for foamed gold. Due to the higher surface areas of the nanostructured electrodes, significantly more of the cefiderocol is oxidised for a similar volume of solution. The local concentration of the target molecule is reduced more quickly, and the maximum peak current becomes limited by diffusion of the analyte from bulk solution. The calibration curves plateau at approximately 100 μM for the carbon nanotube-modified electrodes and at 60 μM for the foamed gold electrode.

Calibrations were repeated in PBS with 4% (w/v) albumin [20]. Fig. 6B and F show slightly enhanced sensitivity compared with carbon

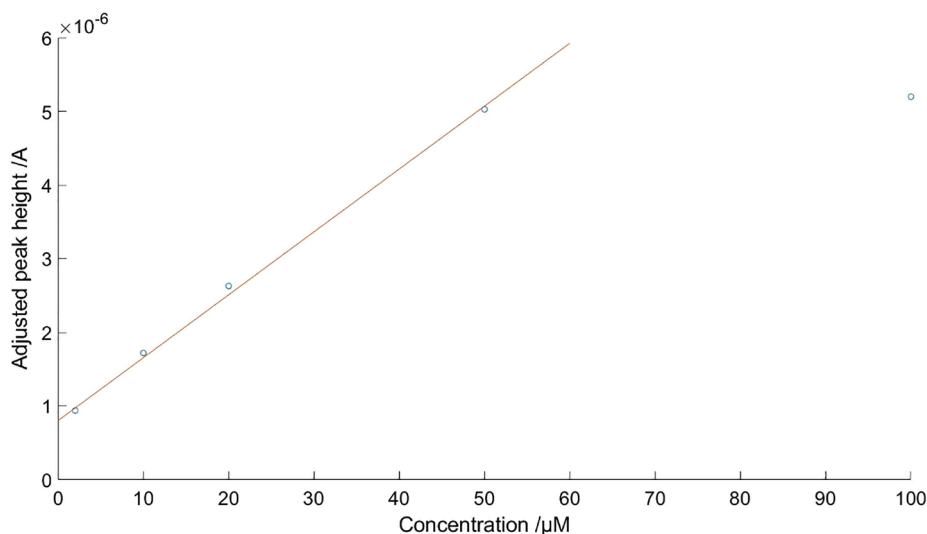


Fig. 7. Calibration of MWCNT screen-printed carbon electrodes in spiked whole human blood: anodic DPV peak height versus cefiderocol concentration.

and gold electrodes in PBS, at 1.24×10^{-3} A/M and 0.134×10^{-3} A/M, respectively. This can be attributed to the catalytic regeneration of cefiderocol by reaction with reduced cysteine groups on albumin. For the carbon nanotube-modified electrodes and foamed gold electrodes (Fig. 6D and H), the sensitivity is slightly reduced relative to the same electrodes in PBS, but still significantly greater than the unmodified electrodes, at 17.4×10^{-3} A/M for carbon nanotubes up to 100 μ M and 8.37×10^{-3} A/M thereafter, and 1.79×10^{-3} A/M for foamed gold electrodes. The reduction in sensitivity is probably due to albumin fouling the electrodes as well as to the approximately 58% protein binding of cefiderocol [32], which makes it unavailable to the electrode nanodomains.

MWCNT-coated pyrolytic carbon electrodes (see supplementary information) were tested on blood samples from healthy volunteers, as a prototype for a clinical point-of-care sensor. 40 μ L of blood were pipetted on, and differential pulse voltammetry was carried out (conditions as above).

Fig. 7 shows a calibration curve for disposable carbon electrodes modified with MWCNT in spiked whole human blood. These have a sensitivity of 88.8×10^{-3} A/M and a theoretical limit of detection of 3.96 μ M. This limit of detection falls below the minimum inhibitory concentration for cefiderocol, and key therapeutic target, of 4 μ M. This demonstrates that this detection method could be used clinically for the therapeutic monitoring of cefiderocol in blood. However, there is notable sensor-to-sensor variability, due predominantly to inconsistent deposition of the MWCNT (see Figs. S3 and S4 in supplementary information). This will need to be addressed before clinical application of these point-of-care sensors.

4. Conclusion

We have demonstrated a novel point-of-care sensor for direct electrochemical detection and quantitation of cefiderocol. Fitness for purpose is demonstrated by a limit of detection below the MIC of cefiderocol and good sensitivity across the therapeutic range. This would allow for effective therapeutic drug monitoring and the optimisation of cefiderocol dosage to ensure blood concentrations remain above the MIC, improving drug efficacy [33], as well as reducing the risk of development of antimicrobial resistance to this drug.

CRedit authorship contribution statement

James McLeod: Writing – original draft, Investigation. Ellen

Stadler: Writing – review & editing, Investigation. Richard Wilson: Resources. Alison Holmes: Supervision. Danny O'Hare: Supervision, Writing – review & editing, Conceptualization.

Declaration of Competing Interest

The authors declare the following financial interests/personal relationships which may be considered as potential competing interests: James McLeod's PhD is in part funded by Shionogi & Co. Ltd, the company responsible for Cefiderocol.

Acknowledgments

JMcL is supported by a studentship from Shionogi and the Medical Research Council through the iCASE doctoral training program. ES is supported by the Swiss European mobility program. AH is affiliated to the National Institute for Health Research Health Protection Research Unit (NIHR HPRU) in Healthcare Associated Infections and Antimicrobial Infections in partnership with Public Health England (PHE), in collaboration with Imperial Healthcare Partners, University of Cambridge and University of Warwick. Additionally, thanks must be given to Centre for Antimicrobial Optimisation (CAMO) Imperial College London (funded by the UK's Department of Health and Social Care), which provided additional financial support, access to infrastructure and assistance with the collection and processing of human blood samples. The authors are grateful to Paul Arkell, a member of CAMO, for assistance with collection of blood samples.

Appendix A. Supplementary data

Supplementary data to this article can be found online at <https://doi.org/10.1016/j.elecom.2021.107147>.

References

- [1] R.I. Aminov, The role of antibiotics and antibiotic resistance in nature, *Environ. Microbiol.* 11 (2009) 2970–2988, <https://doi.org/10.1111/j.1462-2920.2009.01972.x>.
- [2] R.J.W. Lambert, J. Pearson, Susceptibility testing: accurate and reproducible minimum inhibitory concentration (MIC) and non-inhibitory concentration (NIC) values, *J. Appl. Microbiol.* 88 (5) (2000) 784–790, <https://doi.org/10.1046/j.1365-2672.2000.01017.x>.
- [3] C.F. Carson, K.A. Hammer, T.V. Riley, Broth micro-dilution method for determining the susceptibility of *Escherichia coli* and *Staphylococcus aureus* to the essential oil of *Melaleuca alternifolia* (tea tree oil), *Microbios* 82 (1995) 181–185.

- [4] P. Lopez-Vazquez, J.M. Vazquez-Lago, A. Figueiras, Misprescription of antibiotics in primary care: A critical systematic review of its determinants, *J. Eval. Clin. Pract.* 18 (2012) 473–484, <https://doi.org/10.1111/j.1365-2753.2010.01610.x>.
- [5] T.M. Rawson, R.C. Wilson, D. O'Hare, P. Herrero, A. Kambugu, M. Lamorde, M. Ellington, P. Georgiou, A. Cass, W.W. Hope, A.H. Holmes, Optimizing antimicrobial use: challenges, advances and opportunities, *Nat. Rev. Microbiol.* 2021 (2021) 1–12, <https://doi.org/10.1038/s41579-021-00578-9>.
- [6] S. Andrei, G. Droc, G. Stefan, FDA approved antibacterial drugs: 2018–2019, *Discoveries* 7 (4) (2019) e102, <https://doi.org/10.15190/d.2019.15>.
- [7] Home | AMR Review, (n.d.). <https://amr-review.org/home.html> (accessed November 23, 2019).
- [8] E. Charani, M. McKee, R. Ahmad, M. Balasegaram, C. Bonaconsa, G.B. Merrett, R. Busse, V. Carter, E. Castro-Sanchez, B.D. Franklin, P. Georgiou, K. Hill-Cawthorne, W. Hope, Y. Imanaka, A. Kambugu, A.J.M. Leather, O. Mbamalu, M. McLeod, M. Mendelson, M. Mpundu, T.M. Rawson, W. Ricciardi, J. Rodriguez-Manzano, S. Singh, C. Tsioutis, C. Uchea, N. Zhu, A.H. Holmes, Optimising antimicrobial use in humans – review of current evidence and an interdisciplinary consensus on key priorities for research, *Lancet Reg. Heal. - Eur.* 7 (2021) 100161, <https://doi.org/10.1016/j.lanepe.2021.100161>.
- [9] G.G. Zhanel, A.R. Golden, S. Zelenitsky, K. Wiebe, C.K. Lawrence, H.J. Adam, T. Idowu, R. Domalaon, F. Schweizer, M.A. Zhanel, P.R.S. Lagacé-Wiens, A. J. Walkty, A. Noreddin, J.P. Lynch III, J.A. Karlowsky, Cefiderocol: A siderophore cephalosporin with activity against carbapenem-resistant and multidrug-resistant Gram-negative bacilli, *Drugs* 79 (3) (2019) 271–289, <https://doi.org/10.1007/s40265-019-1055-2>.
- [10] J.Y. Wu, P. Srinivas, J.M. Pogue, Cefiderocol: a novel agent for the management of multidrug-resistant Gram-negative organisms, *Infect. Dis. Ther.* 9 (1) (2020) 17–40, <https://doi.org/10.1007/s40121-020-00286-6>.
- [11] H. Li, P. Dauphin-Ducharme, G. Ortega, K.W. Plaxco, Supporting Information for Calibration-free electrochemical biosensors supporting accurate molecular measurements directly in undiluted whole blood, n.d.
- [12] S. Cherevko, C.-H. Chung, Direct electrodeposition of nanoporous gold with controlled multimodal pore size distribution, *Electrochem. Commun.* 13 (1) (2011) 16–19, <https://doi.org/10.1016/j.elecom.2010.11.001>.
- [13] H. Bi, Y. Li, S. Liu, P. Guo, Z. Wei, C. Lv, J. Zhang, X.S. Zhao, Carbon-nanotube-modified glassy carbon electrode for simultaneous determination of dopamine, ascorbic acid and uric acid: The effect of functional groups, *Sensors Actuators B Chem.* 171–172 (2012) 1132–1140, <https://doi.org/10.1016/j.snb.2012.06.044>.
- [14] Glassy Carbon Sensors | redi.bio, (n.d.). <https://www.redi.bio/product-page/glassy-carbon-sensors> (accessed September 7, 2021).
- [15] J.O. Bockris, A.K.N. Reddy, M. Gamboa-Aldeco, *Modern Electrochemistry - Volume 2A, Fundamentals of Electrodes* (2002).
- [16] S. Maldonado, S. Morin, K.J. Stevenson, Electrochemical oxidation of catecholamines and catechols at carbon nanotube electrodes, *Analyst* 131 (2) (2006) 262–267, <https://doi.org/10.1039/B506869J>.
- [17] H. Beiginejad, D. Nematollahi, M. Bayat, F. Varmaghani, A. Nazarpour, Experimental and theoretical analysis of the electrochemical oxidation of catechol and hydroquinone derivatives in the presence of various nucleophiles, *J. Electrochem. Soc.* 160 (10) (2013) H693–H698, <https://doi.org/10.1149/2.037310jes>.
- [18] S. Patai, Z. Rappoport, *The Chemistry of the Quinonoid Compounds*, Wiley (2010), <https://doi.org/10.1002/9780470772119>.
- [19] M. Hasanzadeh, N. Shadjou, Electrochemical nanobiosensing in whole blood: Recent advances, *TrAC - Trends Anal. Chem.* 80 (2016) 167–176, <https://doi.org/10.1016/j.trac.2015.07.018>.
- [20] J.T. Busher, Serum Albumin and Globulin, Chapter 101 in *Clinical Methods: The History, Physical, and Laboratory Examinations*, H.K. Walker, W.D. Hall, J.W. Hurst, Eds, 3rd edition. Boston: Butterworths; 1990. <https://pubmed.ncbi.nlm.nih.gov/21250048/> (accessed September 10, 2021).
- [21] R. Trouillon, D. O'Hare, Comparison of glassy carbon and boron doped diamond electrodes: Resistance to biofouling, *Electrochim. Acta* 55 (22) (2010) 6586–6595, <https://doi.org/10.1016/j.electacta.2010.06.016>.
- [22] R. Trouillon, Z. Combs, B.A. Patel, D. O'Hare, Comparative study of the effect of various electrode membranes on biofouling and electrochemical measurements, *Electrochem. Commun.* 11 (7) (2009) 1409–1413, <https://doi.org/10.1016/j.elecom.2009.05.018>.
- [23] R. Trouillon, D. O'Hare, Y. Einaga, Effect of the doping level on the biological stability of hydrogenated boron doped diamond electrodes, *Phys. Chem. Chem. Phys.* 13 (2011) 5422–5429, <https://doi.org/10.1039/c0cp02420a>.
- [24] A.J. Bard, L.R. Faulkner, *Electrochemical Methods - Fundamentals and Applications* (2001).
- [25] S.N. Prashanth, K.C. Ramesh, J. Seetharamappa, Electrochemical oxidation of an immunosuppressant, Mycophenolate Mofetil, and its assay in pharmaceutical formulations, *Int. J. Electrochem.* 2011 (2011) 1–7, <https://doi.org/10.4061/2011/193041>.
- [26] J.I. Gowda, S.T. Nandibewoor, Electrochemical behavior of paclitaxel and its determination at glassy carbon electrode, *Asian J. Pharm. Sci.* 9 (1) (2014) 42–49, <https://doi.org/10.1016/j.ajps.2013.11.007>.
- [27] E.E.L. Tanner, R.G. Compton, How can electrode surface modification benefit electroanalysis? *Electroanalysis* 30 (7) (2018) 1336–1341, <https://doi.org/10.1002/elan.v30.710.1002/elan.201700807>.
- [28] G.G. Wildgoose, P. Abiman, R.G. Compton, Characterising chemical functionality on carbon surfaces, *J. Mater. Chem.* 19 (2009) 4875–4886, <https://doi.org/10.1039/b821027f>.
- [29] G.P. Keeley, M.E.G. Lyons, The effects of thin layer diffusion at glassy carbon electrodes modified with porous films of single-walled carbon nanotubes, *Int. J. Electrochem. Sci.* 4 (2009) 794–809.
- [30] E. Kätelhön, R.G. Compton, Unscrambling illusionary catalysis in three-dimensional particle-modified electrodes: Reversible reactions at conducting particles, *Appl. Mater. Today* 18 (2020) 100514, <https://doi.org/10.1016/j.apmt.2019.100514>.
- [31] F. Huang, Y. Peng, G. Jin, S. Zhang, J. Kong, Sensitive detection of haloperidol and hydroxyzine at multi-walled carbon nanotubes-modified glassy carbon electrodes, *Sensors* 8 (3) (2008) 1879–1889.
- [32] T. Katsube, R. Echols, T. Wajima, Pharmacokinetic and pharmacodynamic profiles of cefiderocol, a novel siderophore cephalosporin, *Clin. Infect. Dis.* 69 (2019) S552–S558, <https://doi.org/10.1093/CID/CIZ828>.
- [33] G. Wong, F.B. Sime, J. Lipman, J.A. Roberts, How do we use therapeutic drug monitoring to improve outcomes from severe infections in critically ill patients? *BMC Infect. Dis.* 14 (2014) 288, <https://doi.org/10.1186/1471-2334-14-288>.